Article

Light Induced Manganese Oxidation and Long-Lived Charge Separation in a Mn–Ru(bpy)–Acceptor Triad

Magnus Borgstrm, Nizamuddin Shaikh, Olof Johansson, Magnus F. Anderlund, Stenbjrn Styring, Bjrn kermark, Ann Magnuson, and Leif Hammarstrm

J. Am. Chem. Soc., **2005**, 127 (49), 17504-17515• DOI: 10.1021/ja055243b • Publication Date (Web): 17 November 2005

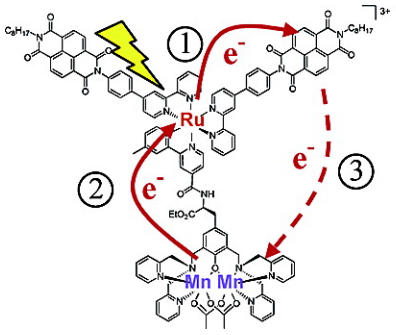

$<\tau_{BET}> \approx 0.5$ s at 140 K

More About This Article

Additional resources and features associated with this article are available within the HTML version:

- Supporting Information
- Links to the 18 articles that cite this article, as of the time of this article download
- Access to high resolution figures
- Links to articles and content related to this article
- Copyright permission to reproduce figures and/or text from this article

View the Full Text HTML

J|A|C|S
ARTICLES
Published on Web 11/17/2005

Light Induced Manganese Oxidation and Long-Lived Charge Separation in a $Mn_2^{II,II}-Ru^{II}(bpy)_3-$Acceptor Triad

Magnus Borgström,[†] Nizamuddin Shaikh,[‡] Olof Johansson,*[,†,§] Magnus F. Anderlund,[§] Stenbjörn Styring,[‡,||] Björn Åkermark,[§] Ann Magnuson,*[,‡] and Leif Hammarström*[,†]

Contribution from the Department of Physical Chemistry, Uppsala University, P.O. Box 579, SE-751 23 Uppsala, Sweden, Department of Molecular Biomimetics, Uppsala University, Villavägen 6, SE-752 36 Uppsala, Sweden, Department of Organic Chemistry, Stockholm University, SE-106 91 Stockholm, Sweden, and Department of Biochemistry, Center for Chemistry and Chemical Engineering, Lund University, P.O. Box 124, SE-221 00 Lund, Sweden

Received August 2, 2005; E-mail: Leif.Hammarstrom@fki.uu.se

Abstract: The photoinduced electron-transfer reactions in a $Mn_2^{II,II}-Ru^{II}-$NDI triad (**1**) ($[Mn_2(bpmp)(OAc)_2]^+$, bpmp = 2,6-bis[bis(2-pyridylmethyl)aminomethyl]-4-methylphenolate and OAc = acetate, Ru^{II} = tris-bipyridine ruthenium(II), and NDI = naphthalenediimide) have been studied by time-resolved optical and EPR spectroscopy. Complex **1** is the first synthetically linked electron donor−sensitizer−acceptor triad in which a manganese complex plays the role of the donor. EPR spectroscopy was used to directly demonstrate the light induced formation of both products: the oxidized manganese dimer complex ($Mn_2^{II,III}$) and the reduced naphthalenediimide ($NDI^{\bullet-}$) acceptor moieties, while optical spectroscopy was used to follow the kinetic evolution of the $[Ru(bpy)_3]^{2+}$ intermediate states and the $NDI^{\bullet-}$ radical in a wide temperature range. The average lifetime of the $NDI^{\bullet-}$ radical is ca. 600 μs at room temperature, which is at least 2 orders of magnitude longer than that for previously reported triads based on a $[Ru(bpy)_3]^{2+}$ photosensitizer. At 140 K, this intramolecular recombination was dramatically slowed, displaying a lifetime of 0.1−1 s, which is comparable to many of the naturally occurring charge-separated states in photosynthetic reaction centra. It was found that the long recombination lifetime could be explained by an unusually large reorganization energy ($\lambda \approx 2.0$ eV), due to a large inner reorganization of the manganese complex. This makes the recombination reaction strongly activated despite the large driving force ($-\Delta G^\circ = 1.07$ eV). Thus, the intrinsic properties of the manganese complex are favorable for creating a long-lived charge separation in the "Marcus normal region" also when the charge separated state energy is high.

Introduction

The natural photosynthetic process of converting light energy into chemical energy first evolved in nature more than 3 billion years ago with the advent of the ancestors of today's photosynthetic reaction centers.[1] One very important reaction center is Photosystem II (PS II) where photoinduced charge separation is coupled to water oxidation and plasto-quinone reduction. The primary charge separation and the secondary charge stabilization reactions in PS II involve a sequence of reactions carried out by a series of protein-bound redox components of varying chemical nature.[2] During water oxidation in PS II, a $CaMn_4$ cluster[3] is oxidized in four consecutive light reactions to catalyze the four-electron oxidation of water, constituting the so-called S-state cycle.[1b,2b] In the final step, molecular oxygen is released and the $CaMn_4$ cluster returns to its most reduced state.

Most of the current efforts in obtaining a suitable structural and functional model for the oxygen evolving complex are limited to the synthesis and characterization of dinuclear, trinuclear, and tetranuclear manganese complexes in various oxidation states.[4] These complexes have helped to some extent to understand the basic properties of the native $CaMn_4$ cluster, the structure of which is not yet fully elucidated. Our own efforts have instead been devoted to mimic the light induced reactions in PS II by coupling a photoactive $[Ru(bpy)_3]^{2+}$ (tris-bipyridine ruthenium(II)) complex to redox active manganese and tyrosine donors and to organic acceptors.[5,6] Many earlier models based on a donor−chromophore−acceptor triad architecture have been designed to mimic charge separation in photosynthetic reaction

[†] Department of Physical Chemistry, Uppsala University.
[‡] Department of Molecular Biomimetics, Uppsala University.
[§] Stockholm University.
[||] Lund University.

(1) (a) Barber, J.; Andersson, B. *Nature* **1994**, *370*, 31−34. (b) Blankenship, R. E. *Molecular Mechanisms of Photosynthesis*; Blackwell Science Ltd., Oxford, UK, 2002.
(2) (a) Barber, J. *Q. Rev. Biophys.* **2003**, *36*, 71−89. (b) Wydrzynski, T.; Satoh, K. *Advances in Photosynthesis and Respiration (Series Ed. Govindjee) Photosystem II: The Water-Plastoquinone Oxido-Reductase in Photosynthesis*; Kluwer Academic Publishers: Dordrecht, the Netherelands, 2005.
(3) (a) Ferreira, K. N.; Iversson, T. M.; Maghlaoui, K.; Barber, J.; Iwata, S. *Science* **2004**, 1831−1838. (b) Kamyia, N.; Shen, J.-R. *Proc. Natl. Acad. Sci.* **2003**, *100*, 98−103. (c) Zouni, A.; Witt, H.-T.; Kern, J.; Fromme, P.; Krauss, N.; Saenger, W.; Orth, P. *Nature* **2001**, *409*, 739−743.
(4) (a) Ruttinger, W.; Dismukes, G. C. *Chem. Rev.* **1997**, *97*, 1−24. (b) Yagi, M.; Kaneko, M. *Chem Rev.* **2001**, *101*, 21−35. (c) Mukhopadhyar, S.; Mandal, S. K.; Beaduri, S.; Armstrong, W. H. *Chem. Rev.* **2004**, *104*, 3981−4026.

10.1021/ja055243b CCC: $30.25

centers, although they have not included manganese-tyrosine donors as in PS II.[7−10] A frequently used chromophore in models of this type is $[Ru(bpy)_3]^{2+}$ due to its stability and advantageous photophysical properties. Earlier triads based on $[Ru(bpy)_3]^{2+}$ have shown charge-separated state lifetimes of, at best, a few hundreds of nanoseconds.[9−11] To successfully mimic PS II, very long-lived intermediate charge-separated states, stable on a time scale of seconds, are required. It would therefore be desirable to increase the lifetime of the charge-separated states in model complexes and to include bound manganese as an electron donor.

In this work we have studied the photoinduced electron-transfer reactions in the $Mn_2^{II,II}$−Ru^{II}−NDI triad, **1** (Figure 1) ($[Mn_2(bpmp)(OAc)_2]^+$, bpmp = 2,6-bis[bis(2-pyridylmethyl)-aminomethyl]-4-methylphenolate and OAc = acetate, Ru^{II} = tris-bipyridine ruthenium(II), and NDI = naphthalenediimide), by time-resolved optical and EPR spectroscopy, following nanosecond laser flash excitation. In a previous publication[6c] we studied the bpmp−Ru^{II}−NDI triad **2** (Figure 1) without manganese coordinated. It was concluded that both the tertiary amine and the hydrogen bonded tyrosine of the bpmp ligand act as electron donors, resulting in the $bpmp^{\bullet+}$−Ru^{II}−$NDI^{\bullet-}$

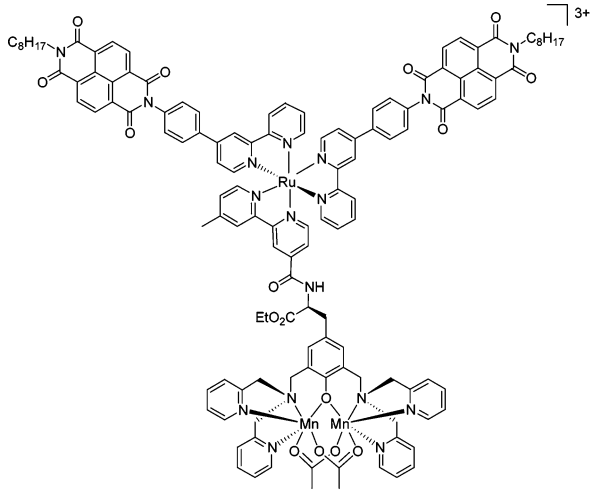

$Mn_2^{II,II}$-Ru^{II}-NDI (**1**)

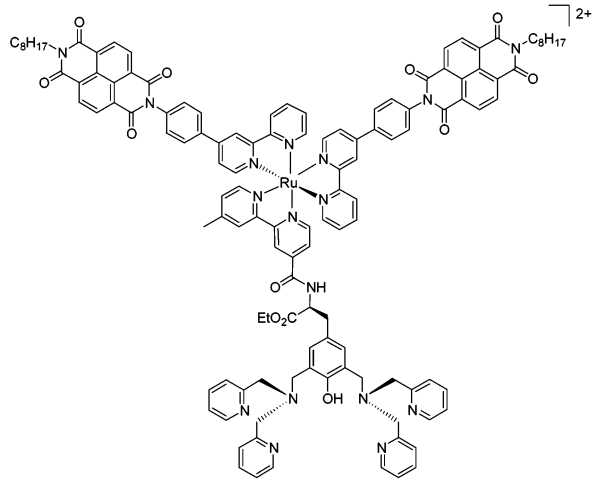

bpmp-Ru^{II}-NDI (**2**)

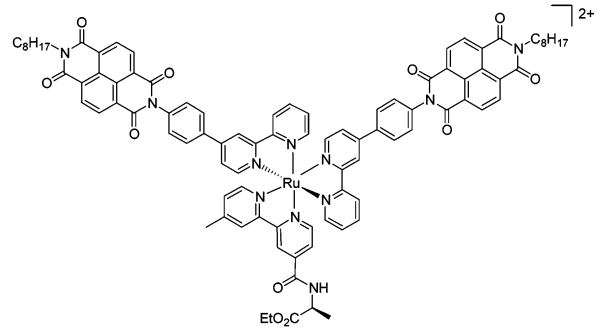

Ala-Ru^{II}-NDI (**3**)

Figure 1. Structure of complexes **1** (the Mn_2-containing triad), **2** (reference compound with bpmp but without coordinated manganese), and **3** (reference compound without the bpmp ligand).

charge-separated state with a quantum yield of ≈10%. By coordinating manganese, the ligand is stabilized resulting in a manganese metal-centered primary electron donor, consistent with electrochemical data.[12,13]

We have earlier shown that $[Mn_2(bpmp)(OAc)_2]^+$ can act as a rapid electron donor in a system similar to **1** but with an external electron acceptor instead of covalently linked NDI.[13,14]

(5) (a) Sun, L.; Hammarström, L.; Åkermark, B.; Styring, S. *Chem. Soc. Rev.* **2001**, *30*, 36−49. (b) Hammarström, L.; Sun, L.; Åkermark, B.; Styring, S. *Spectrochim. Acta A.* **2001**, *37*, 2145−2160. (c) Hammarström, L. *Curr. Opin. Chem. Biol.* **2003**, *7*, 666−673. (d) Magnuson, A.; Styring, S.; Hammarström, L. In *Photosystem II: The water: plastoquinone oxi-doreductase in photosynthesis*; Wydrzynski, T., Satoh, K., Eds.; Kluwer Publications: 2005, in press. (e) Lomoth, R.; Magnuson, A.; Sjödin, M.; Huang, P.; Styring, S.; Hammarström, L. *Photosynth. Res.*, accepted.

(6) (a) Borgström, M.; Johansson, O.; Lomoth, R.; Baudin, H. B.; Wallin, S.; Sun, L.; Åkermark, B.; Hammarström, L. *Inorg. Chem.* **2003**, *42* (17), 5173−5184. (b) Johansson, O.; Borgström, M.; Lomoth, R.; Palmblad, M.; Bergquist, J.; Hammarström, L.; Bergquist, J.; Sun, L.; Åkermark, B. *Inorg. Chem.* **2003**, 2908−2918. (c) Johansson, O.; Wolpher, H.; Borgström, M.; Hammarström, L.; Bergquist, J.; Sun, L.; Åkermark, B. *Chem. Commun.* **2004**, 194−195.

(7) (a) Wasielewski, M. R. *Chem. Rev.* **1992**, *92*, 435−461. (b) Gust, D.; Moore, T. A.; Moore, A. L. *Acc. Chem. Res.* **2001**, *34*, 40−48. (c) Gust. D.; Moore, T. A.; Moore, A. L.; Covalently Linked Systems Containing Porphyrine Units. In *Electron Transfer in Chemistry*; Balzani, V., Ed.; Wiley-VCH: Wennheim, 2001; pp 272−336.

(8) (a) Imahori, H. *Org. Biomol. Chem.* **2004**, *2*, 1425−1433. (b) Guldi, D. M.; Imahori, H.; Tamaki, K.; Kashiwagi, Y.; Yamada, H.; Sakata, Y.; Fukuzumi, S. *J. Phys. Chem. A* **2004**, *108*, 541−548.

(9) (a) Sauvage, J.-P.; Collin, J.-P.; Chambron, J.-C.; Guillerez, S.; Coudret, C.; Balzani, V.; Barigelletti, F.; De Cola, L.; Flamigni, L. *Chem. Rev.* **1994**, *94*, 993−1019. (b) Scandola, F.; Chiorboli, C.; Indelli, M. T.; Rampi, M. A. In *Electron Transfer in Chemistry*; Balzani, V., Ed.; Wiley-VCH: Wennheim, 2001; pp 337−408. (c) Baranoff, E.; Collin, J.-P.; Flamigni, L.; Sauvage, J.-P. *Chem. Soc. Rev.* **2004**, *33*, 147−155.

(10) (a) Cooley, L. F.; Larson, S. L.; Elliott, C. M.; Kelley, D. F. *J. Phys. Chem.* **1991**, *95*, 10694−10700. (b) Huynh, M. H. V.; Dattelbaum, D. M.; Meyer, T. J. *Coord. Chem. Rev.* **2005**, *249*, 457−483. (c) Danielson, E.; Elliott, C. M.; Merkert, J. W.; Meyer, T. J. *J. Am. Chem. Soc.* **1987**, *109*, 2519−2520. (d) Mecklenburg, S. L.; McCafferty, D. G.; Schoonover, J. R.; Peek, B. M.; Erickson, B. W.; Meyer, T. J. *Inorg. Chem.* **1994**, *33*, 2974−2983.

(11) (a) Treadway, J. A.; Chen, P.; Rutherford, T. J.; Keene, F. R.; Meyer, T. J. *J. Phys. Chem. A* **1997**, *101*, 6824−6826. (b) Opperman, K. A.; Mecklenburg, S. L.; Meyer, T. J. *Inorg. Chem.* **1994**, *33*, 5295−5301. (c) Maxwell, K. A.; Sykora, M.; DeSimone, J. M.; Meyer, T. J. *Inorg. Chem.* **2000**, *39*, 71−75. (d) Klumpp, T.; Limsemann, M.; Limoges, B. R.; Burssner, D.; Krissinel, E. B.; Elliot, C. M.; Steiner, U. E. *J. Am. Chem. Soc.* **1999**, *121*, 1076−1097. (e) Larson, S. L.; Elliott, C. M.; Kelley, D. F. *J. Phys. Chem.* **1995**, *99*, 6530−6539. (f) Chiorboli, C.; Fracasso, S.; Scandola, F.; Campagna, S.; Serroni, S.; Konduri, R.; MacDonnell, F. M. *Chem. Commun.* **2003**, *14*, 1658−1659. (g) A family of $[Ru(bpy)_3]^{2+}$-viologen pseudo-rotaxanes has been reported to give an intramolecular charge separation half-life for the Ru^{III}−$MV^{\bullet+}$ of ca. 200 μs in all cases, due to complexation with a supposedly redox-inert macrocycle (Duerr, H.; Bossman, S. *Acc. Chem. Res.* **2001**, *34*, 905−917). However, the macrocycle contained an electron donor with a formal potential only slightly above that for the $Ru^{III/II}$ couple. As the macrocylce was added in large excess it should, contrary to the authors' assumptions, reduce the photo-oxidized Ru^{III} quantitatively under the experimental conditions. Thus, it is likely that the observed viologen radical decay was instead due to a trivial bimolecular recombination with oxidized, external macrocycles (i.e., not threaded on the rotaxane), for which a ca. 200 μs half-life can be expected with the typical concentrations generated in the laser flash experiments.

In that study we observed fast intramolecular electron transfer ($\tau < 100$ ns), from the manganese dimer to the photo-oxidized Ru^{III}, limited by the initial reaction with the external electron acceptor.[13] We could also demonstrate sequential, three-step oxidation of the manganese dimer, bringing it from $Mn_2^{II,II}$ to $Mn_2^{III,IV}$, in experiments where a sacrificial electron acceptor in aqueous solution was used.[14] This multistep manganese oxidation also involved the charge-compensating exchange of the acetate ligands for water-derived ligands, which in the $Mn_2^{III,IV}$ state appeared as two oxo-bridges between the two manganese ions.[15] Thus, complex **1** contains both a manganese moiety able to perform multistep electron transfer and two covalently linked NDI acceptors able to act as electron acceptors. Complex **1** should therefore be a promising candidate to mimic light-induced charge separation involving the manganese cluster in PS II.

Below we show how photoexcitation of **1** results in a very long-lived charge-separated state detectable by both optical and EPR spectroscopy. Importantly, for the long-lived charge separation at 140 K, we could detect and follow the recombination of both products, viz. the $NDI^{\bullet-}$ and the $Mn^{II,III}$.

Experimental Section

All liquid phase measurements were performed in Ar-purged butyronitrile (Fluka) dried over molecular sieves, except otherwise noted. Some transient absorption experiments were also performed in butyronitrile distilled over P_2O_5. Room-temperature transient absorption was also performed in acetonitrile (Aldrich, spectroscopic grade, dried over molecular sieves). Acetonitrile was also used for the time-correlated single photon counting experiments because a short-lived emission from an impurity in butyronitrile overlapped with the ruthenium emission. The PMMA (poly(methyl metacrylate; Aldrich) films used in the solid matrix measurements were prepared by dissolving the dyes in a solution of PMMA dissolved in CH_2Cl_2 (Aldrich, spectroscopic grade) and thereafter evaporating the CH_2Cl_2.

Optical Spectroscopy. Electronic absorption spectra were recorded on an UV/vis diode array spectrophotometer (Hewlett-Packard 8435), and emission spectra were recorded on an SPEX-Flourolog II system using 1 cm quartz cuvettes. The time correlated single photon counting setup has been described previously.[6b] The emission was collected at magic angle polarization (55.4°) relative to the excitation light. The response function of the instruments was ≈60 ps. Also the flash photolysis setup has been described earlier.[6b] All transient absorption experiments used 455 nm excitation light. The energy per pulse was ≈15 mJ and the pulse width < 10 ns. For the measurements below 298 K we used a variable temperature liquid nitrogen cryostat, DN1704. The temperature was set with an ITC601 temperature controller (Oxford Instruments). Unless indicated otherwise, the concentration of the solute was ≈20 μM.

EPR Spectroscopy. X-band EPR measurements were performed on a Bruker E580-ELEXYS spectrometer equipped with a Bruker ER 4116D dual mode resonator or a Bruker ER ST4102 Standard Cavity (both accessible for incident illumination). The temperature was regulated with an ITC 503 temperature controller in an ESR 900 flow cryostat from Oxford Instruments. Data analysis was carried out with the Bruker Xepr software, version 2.1. A liquid nitrogen flow system (Model TC1 Variable Temperature Controller from Wilmad) was sometimes used to achieve 140 K in the laser flash experiments. Laser flashes at 532 nm (6 ns pulse width, 250 mJ/flash, 5 Hz) were provided to the samples from a Spectra Physics DCR 3G Nd:YAG laser. Flashes at 460 nm were provided via a Quanta Ray MOPO-730 OPO providing ca. 20 mJ/flash in the EPR cavity.

The EPR samples were prepared in complete darkness to avoid any unwanted light reactions. 100 μL of the solvated samples of **1** in butyronitrile were transferred to EPR tubes and rapidly cooled to 77 K. Laser flashes were provided, either directly to the EPR samples in the EPR cavity or to the EPR sample inserted in a non-silvered dewar cooled to the appropriate temperature with nitrogen gas. The incident laser light was adjusted with lenses so that the entire sample volume was covered during illumination. When laser flashing was performed outside the EPR cavity, the EPR tubes were transferred to liquid N_2 (77 K) by hand after the designated number of laser flashes. This sample transfer, occurring in complete darkness, took 2−3 s to complete. The X-band EPR spectra were recorded both before and after the flash illumination of the EPR samples.

Quantification of the various species formed in the photochemical experiments ($Mn_2^{II,II}$, $Mn_2^{II,III}$, and the $NDI^{\bullet-}$ radical) were achieved with standard samples measured under identical conditions as those used for the EPR samples of **1** in the experiments. $[Mn_2(bpmp)(OAc)_2]^{+}$ [13] was used as $Mn_2^{II,II}$ reference. To calculate the contribution of $Mn_2^{II,II}$ to the EPR spectra of **1**, the EPR spectrum of the standard $Mn_2^{II,II}$ was recorded at 11 K. The area under the spectral feature around 2600 G, which belongs to the EPR spectrum from the $Mn_2^{II,II}$ form,[16] was double integrated (marked with double headed arrow in Figure 3 spectrum (i)). For the estimation of the $Mn_2^{II,III}$ concentration, the EPR spectrum of a standard sample of $[Mn_2(bpmp)(OAc)_2]^{2+}$ [12] was recorded at 4 K. The area under the ground state ($S = {}^1/_2$) EPR spectrum was double integrated to calculate the concentration. The EPR spectra of **1** were then recorded under the same conditions to analyze the content of $Mn_2^{II,II}$ and $Mn_2^{II,III}$ in each sample of **1** before and after the flash illumination.

For quantification of the $NDI^{\bullet-}$ radical, we used the stable $Tyrosine_D$ radical in Photosystem II ($Tyr_D^{\bullet}$), recorded under nonsaturating conditions as spin standard. $Tyr_D^{\bullet}$ amounts to one radical per PSII reaction center, and its concentration can be calculated accurately on a chlorophyll/PS II reaction center basis.[17] The concentration of the $NDI^{\bullet-}$ radical was estimated from its EPR spectrum, recorded under the same nonsaturating conditions, and compared to the EPR spectrum from $Tyr_D^{\bullet}$. We estimate the accuracy in the concentration determinations from the EPR spectra to be ±5% for the $Mn_2^{II,II}$ and the radical EPR spectra and to be ±15% for the EPR spectrum from $Mn_2^{II,III}$.

Synthesis. $Mn_2^{II/II}-Ru^{II}-NDI$ (**1**). The bpmp−Ru^{II}−NDI precursor[6c] (0.040 g, 1.6×10^{-5} mol) and $Mn^{II}(OAc)_2$ (0.010 g, 4×10^{-5} mol) were dissolved in a degassed CH_3CN/EtOH mixture (1:9, 1.5 mL) and heated at 80 °C under an argon atmosphere in the dark for 15 min. An aqueous solution of ammonium hexafluorophosphate (0.013 g in 0.5 mL H_2O) was added dropwise, and the mixture was cooled to 0 °C. The precipitate was filtered off and washed with H_2O and Et_2O and dried under vacuum (0.028 g, 61%).

ESI-FTICR MS (*m*/*z*): $[M - 2PF_6^-]^{2+}$ 1258.92 (calcd for $C_{129}H_{118}Mn_2N_{17}O_{16}Ru\,PF_6$: 1258.82), $[M - 3PF_6^-]^{3+}$ 790.95 (calcd for $C_{129}H_{118}Mn_2N_{17}O_{16}Ru$: 790.89).

(12) (a) Diril, H.; Chang, H. R.; Zhang, X.; Larsen, S. K.; Potenza, J. A.; Pierpont, C. G.; Schugar, H. J.; Isied, S. S.; Hendrickson, D. N. *J. Am. Chem. Soc.* **1987**, *109*, 6207−6208. (b) Diril, H.; Chang, H.-R.; Nilges, M. J.; Zhang, X.; Potenza, J. A.; Schugar, H. J.; Isied, S. S.; Hendrickson, D. N.; *J. Am. Chem. Soc.* **1989**, *111*, 5102−5114.
(13) Sun, L.; Raymond, M.; Magnuson, A.; LeGourrierec, D. Tamm, M.; Abrahamsson, M.; Huang Kenez, P.; Mårtensson, J.; Stenhagen, G.; Hammarström, L.; Almgren, M.; Styring, S.; Åkermark, B. *J. Inorg. Biochem.* **2000**, *78*, 15−22.
(14) Huang, P.; Magnuson, A.; Lomoth, R.; Abrahamsson, M.; Tamm, M.; Sun, L.; van Rotterdam, B.; Park, J.; Hammarström, L.; Åkermark, B.; Styring, S. *J. Inorg. Biochem.* **2002**, *91*, 159−172.
(15) Eilers, G.; Zettersten, C.; Nyholm, L.; Hammarström, L.; Lomoth, R. *Dalton Trans.* **2005**, 1033−1041.
(16) (a) Blanchard, S.; Blondin, G.; Riviere, E.; Nierlich, M.; Girerd, J.-J. *Inorg. Chem.* **2003**, *42*, 4568−4578. (b) Blanchard, S.; Blain, G.; Riviere, E.; Nierlich, M.; Blondin, G. *Chem.−Eur. J.* **2003**, *9*, 4260−4268.
(17) (a) Babcock, G. T.; Sauer, K. *Biochim. Biophys. Acta* **1973**, *325*, 483−503. (b) Miller, A.-F,; Brudvig, G. W. *Biochim. Biophys. Acta* **1991**, *1056*, 1−18. (c) Rutherford, A. W.; Boussac, A.; Faller, P. *Biochim. Biophys. Acta* **2004**, *1655*, 222−230.

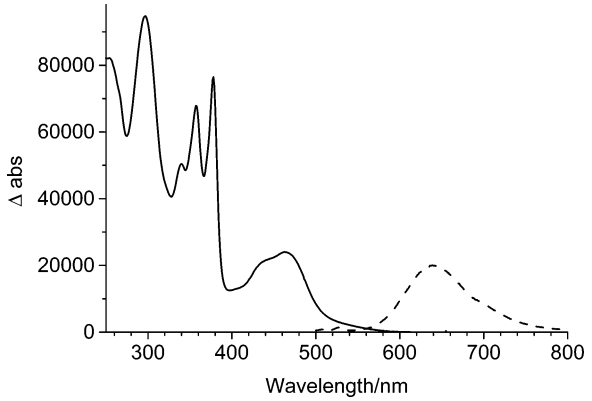

Figure 2. UV−vis absorption spectrum (—) and emission spectrum (- - -) of **1** recorded in butyronitrile at 298 K.

Elemental analyses calcd (%) for $C_{129}H_{118}Mn_2N_{17}O_{16}RuP_3F_{18}\cdot 3H_2O$: C, 54.13; H, 4.37; N, 8.32. Found: C, 54.10; H, 4.37; N, 8.30.

Results and Discussion

Synthesis and Characterization. A. Synthesis. The $Mn_2^{II/II}$–Ru^{II}–NDI triad **1** was prepared from the bpmp–Ru^{II}–NDI precursor **2**[6c] and $Mn^{II}(OAc)_2$ in a CH_3CN/EtOH mixture under an argon atmosphere in the dark. Electrospray mass spectrometry verified the molecular mass of the triad **1**, with observed peaks at 1258.9 ($\mathbf{1}^{2+}$) and 790.9 ($\mathbf{1}^{3+}$) corresponding to the loss of two and three PF_6^- counterions, respectively. Furthermore, the purity of **1** was confirmed by elemental analyses, which was in perfect agreement with the expected values.

When preparing donor–sensitizer–acceptor assemblies based on $[Ru(bpy)_3]^{2+}$, where the donor and acceptor are attached to different 2,2'-bipyridines, a mixture of geometrical isomers is normally obtained. The possible existence of isomers has usually been acknowledged in previously studied $[Ru(bpy)_3]^{2+}$-based chromophore-quencher assemblies, and the electron transfer kinetics observed following excitation has been treated as an average for the isomers (see, e.g., refs 6a,11b). Recently, Keene and co-workers successfully separated the four possible geometric isomers of a donor–sensitizer–acceptor triad using a combination of fractional crystallization and cation-exchange chromatography[18] and reported distinctly different electron transfer rate constants for all isomers.[11a] In the triad **1**, containing two naphthalenediimide acceptors and one $Mn_2^{II,II}$ donor, four geometrical isomers are possible,[19] and it is assumed that a statistical mixture of the various forms was isolated. It is interesting to note that a trans relationship between the donor and one acceptor is present in only two out of four isomers, while all four isomers have one or two cis relationships.

B. Absorption and Emission Spectra. The UV−vis absorption spectrum of **1** (Figure 2) showed typical features from the $[Ru(bpy)_3]^{2+}$ unit with a metal-to-ligand charge transfer (MLCT) band at 462 nm and strong $\pi-\pi^*$ transitions in the UV region at 296 and 235 nm.[20] In addition, strong $\pi-\pi^*$ transitions from the NDI moieties are apparent at 378, 358, and 340 nm.[21] The spectrum is very similar to the reference complex **2** which does not contain manganese.[6c] This is expected since the $[Mn_2(bpmp)(OAc)_2]^+$ unit shows negligible absorption in the visible region.[12,13]

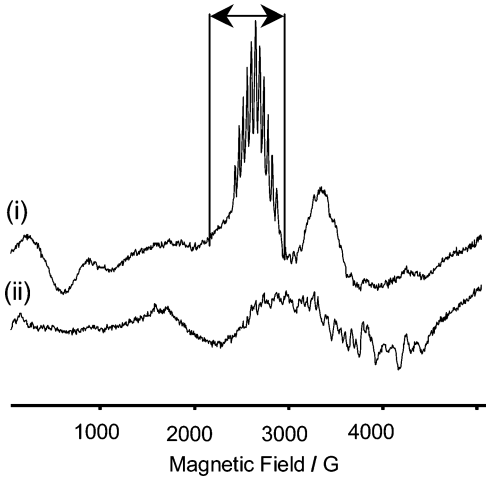

Figure 3. X-band EPR spectra of **1** (0.71 mM) recorded in butyronitrile in the dark at (i) 11.2 K and (ii) 4.3 K. The feature between the arrows in (i) is an 11-line feature originating from $Mn_2^{II,II}$. Each spectrum is the average of four scans. EPR settings: microwave frequency, 9.62 GHz; modulation amplitude, 10 G; microwave power, 10 mW.

The emission spectrum of **1** at room temperature peaked at 640 nm (uncorrected spectrum, Figure 2), and the spectral feature resembles the emission of $[Ru(bpy)_3]^{2+}$ ($\lambda_{max} = 608$ nm). The emission intensity of **1** was quenched by 95% as compared to $[Ru(bpy)_3]^{2+}$ due to the presence of the attached NDI and $Mn_2^{II,II}$ unit (see below). The energy of the excited triplet state was assumed to be equal to that of the reference **2** ($E_{00} = 2.05$ eV). This value was estimated from the highest energy vibrational band of a 77 K emission spectrum. Earlier studies have shown that this is a good approximation.[22]

C. EPR Spectra in the Dark. The EPR spectra from **1** prior to any light excitation are shown in Figure 3. The spectrum, recorded at 11 K, is more than 5000 G wide, typical of the two weakly coupled manganese ions in the $Mn_2^{II,II}$ complex.[14,16] Two of the prominent spectral features are the well resolved 11-line ^{55}Mn hyperfine structure with a splitting constant of ca. 45 G centered at 2600 G (marked with arrows in Figure 3 spectrum (i)) and a broad transition centered at 3640 G. Both features are typical of a spin coupled $Mn_2^{II,II}$ dimer, and the observed transitions are due to the superposition of several spin state signatures.[14,16,23] Antiferromagnetic coupling between two high spin Mn^{II} ions ($S = {}^5/_2$) leads to a diamagnetic ground state and paramagnetic excited states with integer spin values ranging from 1 to 5. The transitions observed at 11 K in X-band are therefore attributed to several excited states, and the spectrum is well understood.

When the spectrum was measured at 4 K, only the diamagnetic ground state from the $Mn_2^{II,II}$ pair is significantly populated and the intensity of the 11-line feature around 2600 G is reduced.

(18) Keene, F. R. *Coord. Chem. Rev.* **1997**, *166*, 121−159.
(19) As well as geometrical isomers, several diastereomeric forms are possible due to the additional stereogenic centres in the triad.
(20) (a) Juris, A.; Balzani, V.; Barigelletti, F.; Campagna, S.; Belser, P.; Zelewsky, A. *Coord. Chem. Rev.* **1988**, *84*, 85−227. (b) Kalyanasundaram, K. *Photochemistry of Polypyridine and Porphyrin Complexes*; Academic Press: London, 1992.
(21) Barros, T. C.; Brochsztain, S.; Toscano, V. G.; Filho, P. B.; Politi, M. J. *J. Photochem. Photobiol. A: Chem.* **1997**, *111*, 97−104.
(22) (a) Caspar, J. V.; Meyer, T. J. *Inorg. Chem.* **1983**, *22*, 2444−2453. (b) Treadway, J. A.; Loeb, B.; Lopez, R.; Anderson, P. A.; Keene, F. R.; Meyer, T. J. *Inorg. Chem.* **1996**, *35*, 2242−2246. (c) Hammarström, L.; Barigeletti, F.; Flamigni, L.; Indelli, M. T.; Armaroli, N.; Calogero, G.; Guardigli, M.; Sour, A.; Collin, J.-P.; Sauvage, J.-P. *J. Phys. Chem. A* **1997**, *101*, 9061−9069.
(23) Khangulov, S. V.; Pessiki, P. J.; Barynin, V. V.; Ash, D. E.; Dismukes, G. C. *Biochemistry* **1995**, *34*, 2015−2025.

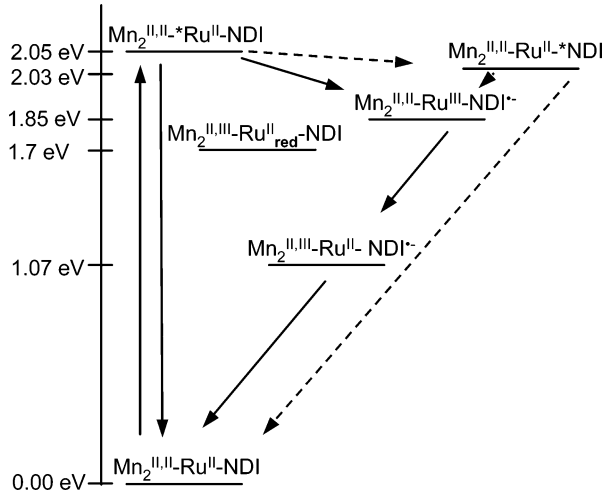

Figure 4. Energy diagram for the different locally excited states (marked with an asterisk) and charge separated states of **1**. The triplet NDI (*NDI) state was only observed in a PMMA matrix at $T < 120$ K (see below). The state involving the reduced Ru^{II} center, formally $Ru^{II}(bpy^{\bullet-})(bpy)_2$ and here denoted Ru^{II}_{red}, was not observed and probably not involved under any of our experimental conditions.

Instead, another 16-line, broad EPR signature becomes prominent (Figure 3(ii)). Albeit small, this signal can be identified as the $Mn_2^{II,III}$ complex, and the spectrum has been reported previously.[12,24] Quantitative estimation (see Experimental Section) suggests that the amount of the $Mn_2^{II,III}$ form is ca. 10% of the total amount of **1**. Importantly we found no evidence of uncoupled Mn(II) in the EPR spectrum showing that the triad **1** is stable in butyronitrile.

D. Redox Potentials and Energetics of Electron Transfer. The reduction potentials for **1** were estimated from the electrochemical data of **2** with $E_{1/2} = +0.88$ V ($Ru^{3+/2+}$) and $E_{1/2} = -0.97$ V ($NDI^{0/-}$) (all vs $Fc^{+/0}$)[6c] and the $Mn_2^{II,II}-Ru^{II}$ dyad lacking the NDI unit with $E_{1/2} = +0.10$ V ($Mn_2^{II,III/II,II}$), $E_{1/2} = +0.63$ V ($Mn_2^{III,III/II,III}$), and $E_{1/2} = -1.6$ V ($[Ru(bpy)_3]^{2+/+}$) (all vs $Fc^{+/0}$).[14,15] Based on these data, together with the triplet excited state energies of **1**, $E_{00} = 2.05$ eV for ruthenium and $E_{00} = 2.03$ eV for NDI,[25] the energy diagram in Figure 4 was drawn (columbic interactions were neglected).

Light Induced Electron Transfer. The idea behind the synthesis of **1** was to study the intramolecular electron transfer reactions. Analogous to the case in complex **2**, photoexcitation of the $[Ru(bpy)_3]^{2+}$ unit should lead to the transfer of an electron to one of the NDI acceptor units,[6c] forming the primary charge separated state $Mn_2^{II,II}-Ru^{III}-NDI^{\bullet-}$. Subsequently the charge pair can either recombine or be further separated by shifting of the electron hole from the Ru^{III} to the $Mn_2^{II,II}$ unit. This would lead to a secondary charge pair with a hole on the manganese donor side ($Mn_2^{II,III}$) and an electron on an NDI unit. With transient optical spectroscopy the kinetics and order of events in the light-induced electron transfer sequence can be followed by monitoring the $NDI^{\bullet-}$ radical and the redox states of the ruthenium photosensitizer, while the manganese dimer is inaccessible due to the low extinction coefficients of both the $Mn_2^{II,II}$ and $Mn_2^{II,III}$ complex units in the visible region.[12,13] With EPR spectroscopy instead, both the anticipated redox states of the manganese dimer and the radical state of NDI are distinguishable and their concentrations are possible to quantify, thus enabling a direct identification of the species involved in the fully charge separated state and the monitoring of their recombination.

A. EPR Spectroscopy. EPR analysis of the Mn_2 unit in **1** can only be done at cryogenic temperatures (4−15 K) while reactions involving the NDI acceptor can be studied at any temperature (both with EPR and optical spectroscopy). First we attempted to study the flash induced changes in **1** by direct laser flashing into the EPR cavity at 4−10 K, which could permit direct observation of redox changes in the manganese dimer. However, at these temperatures we were unable to observe any reaction involving the $Mn_2^{II,II}$ moiety in **1**. We therefore turned to more elevated temperatures where light-induced electron transfer reactions involving manganese might occur. Thus, concentrated EPR samples kept at a defined temperature were irradiated with ns-laser flashes and then transferred by hand to liquid nitrogen, vitrifying the butyronitrile, and further transferred to the EPR cavity. No change in EPR signals occurred in the dark in the vitrified solution on the time scale of experiments and analysis, thus allowing us to trap and quantify long-lived photoproducts. The procedure only allows trapping of states more long-lived than 2 to 3 s.[26]

The photoinduced reactions in the triad were studied at 140 K, where butyronitrile is still liquid. Light-induced electron-transfer reactions were found to occur at this temperature, forming products long-lived enough to trap for EPR analysis as described above. The EPR spectra from samples of **1** exposed to varying numbers of laser flashes at 140 K are shown in Figure 5. Figure 5a and c show the spectra recorded at 11 K to optimize analysis of $Mn_2^{II,II}$ and the $NDI^{\bullet-}$ radical, respectively, and Figure 5b shows the spectra recorded at 4 K to optimize analysis of $Mn_2^{II,III}$.

After 50 flashes, the signal intensity of $Mn_2^{II,II}$ had decreased by 10% concomitantly with an increase of the $Mn_2^{II,III}$ signal (Figure 5a and b). In addition a narrow signal from a radical appeared in the $g = 2$ region (Figure 5c). Note that the EPR spectra in Figure 5a and b are recorded under spectral conditions which are optimized for analysis of changes in the manganese moiety and they are not optimal for analysis of the radical. Instead, EPR spectra recorded under optimal conditions for the radical (Figure 5c) revealed this signal was ca. 8 G wide from peak to trough with a g-value of 2.0107, typical for the $NDI^{\bullet-}$ radical.[27] Continued laser flashing of the sample resulted in a further decrease of $Mn_2^{II,II}$ and an increase of $Mn_2^{II,III}$ as well as an increase of the $NDI^{\bullet-}$ radical signal (spectrum after 250 flashes shown in Figure 5). Figure 6 shows that after 50 flashes 0.06 mM of $Mn^{II,II}$ had been oxidized, after 250 flashes 0.19 mM of $Mn^{II,II}$ was oxidized, and after 500 flashes 0.20 mM of $Mn^{II,II}$ was oxidized, which corresponds to ca. 32% of the sample. In the same experiment, the increase in $Mn_2^{II,III}$ was found to be 0.04 mM, 0.09 mM, and 0.11 mM, respectively. It

(24) Huang, P.; Högblom, J.; Anderlund, M. F.; Sun, L.; Magnuson, A.; Styring, S. *J. Inorg. Biochem.* **2004**, *98*, 733−745.
(25) (a) Green, S.; Fox, M. A. *J. Phys. Chem.* **1995**, *99*, 2−14757. (b) Roger, J. E.; Kelly, L. A. *J. Am. Chem. Soc.* **1999**, *121*, 3854−3861.
(26) It should be noted that "normal" rapid-feeze methods for EPR spectroscopy, using fast mixing techniques and quenching in liquid isopentane or similar, are not easily performed using strong laser flash excitation in a laboratory that is otherwise completely dark. We are aware of only one such attempt, and freezing times below several hundred milliseconds could not be achieved despite flashing very close to the isopentane surface; see: Boussac, A.; Rutherford, A. W.; Styring, S. *Biochemistry* **1990**, *29*, 24−32.
(27) Brochsztain, S.; Rodrigues, M. A.; Demets, G. J. F.; Politi, M. J. *J. Mater. Chem.* **2002**, *12*, 1250−1255.

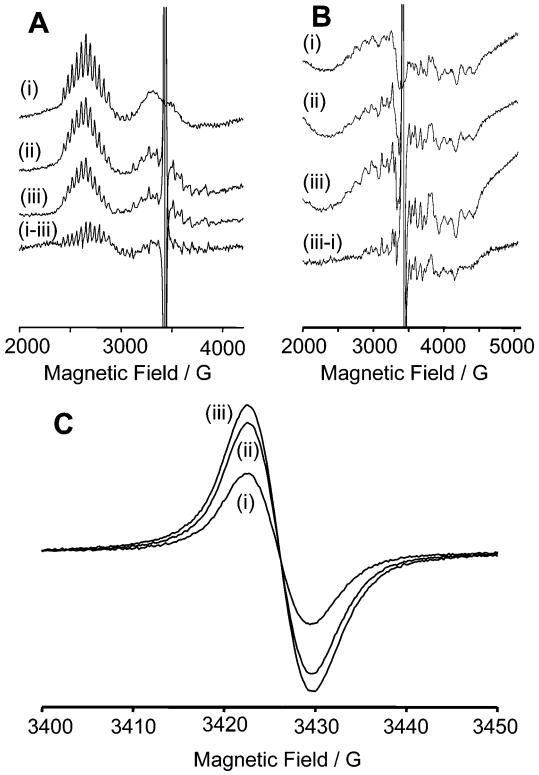

Figure 5. EPR spectra of **1** recorded at 11 K (panels a and c) or 4 K (panel b) in the (i) dark, after (ii) 50 flashes and (iii) 250 flashes given to the sample at 140 K. Spectrum (i-iii) in panel a is the difference spectrum showing the decrease of the $Mn_2^{II,II}$ after 250 flashes, and spectrum (iii-i) in panel b shows the corresponding increase in $Mn_2^{II,III}$. Each spectrum is the average of four scans. Panel c shows the EPR spectra of the $NDI^{\bullet-}$ radical recorded during the same 140 K flash photolysis experiment after (i) 50 flashes, (ii) 150 flashes, and (iii) 500 flashes. It should be noted that the spectrum in the dark did not contain any EPR signal from the $NDI^{\bullet-}$ radical (not shown). Each spectrum is the average of 8 scans. All EPR spectra are recorded in the same sample given different numbers of flashes. [**1**] = 0.71 mM, solvent butyronitrile. EPR spectrometer settings: microwave frequency, 9.62 GHz; modulation amplitude = 10 G; receiver gain = 65 dB; microwave power = 10mW in panels A and B and 0.2 mW in panel C.

might seem that the formation of $Mn_2^{II,III}$ was lower than the decrease in $Mn_2^{II,II}$. However, the EPR spectrum from $Mn_2^{II,III}$ is more difficult to quantify than the spectrum from $Mn_2^{II,II}$, and our error is larger (see Experimental Section). In particular this holds for the spectra where the $NDI^{\bullet-}$ radical overlaps the spectrum from $Mn_2^{II,III}$.

The formation of the $NDI^{\bullet-}$ radical followed stoichiometrically the oxidation of $Mn_2^{II,II}$, within experimental accuracy. Thus after 50 flashes, the formed $NDI^{\bullet-}$ radical amounted to 0.07 mM, which should be compared to the oxidation of $Mn_2^{II,II}$ (0.06 mM). After 500 flashes the concentration of the $NDI^{\bullet-}$ radical was 0.22 mM while the total decrease in $Mn_2^{II,II}$ was 0.20 mM. Thus, the observed concentration changes originate, at least predominantly, from the light driven charge separation between the $Mn_2^{II,II}$ moiety and the NDI acceptor in **1** according to eq 1.

$$Mn_2^{II,II}-Ru^{II}-NDI \rightarrow Mn_2^{II,III}-Ru^{II}-NDI^{\bullet-} \qquad (1)$$

It should be noted that ca. 10% of **1** is present as the $Mn_2^{II,III}$ form (Figure 3) from the start. It is thermodynamically feasible that these molecules might also give a light-induced charge separation. This would form $Mn_2^{III,III}$, which is EPR silent, and result in oxidation of a part of the $Mn_2^{II,III}$ complexes present

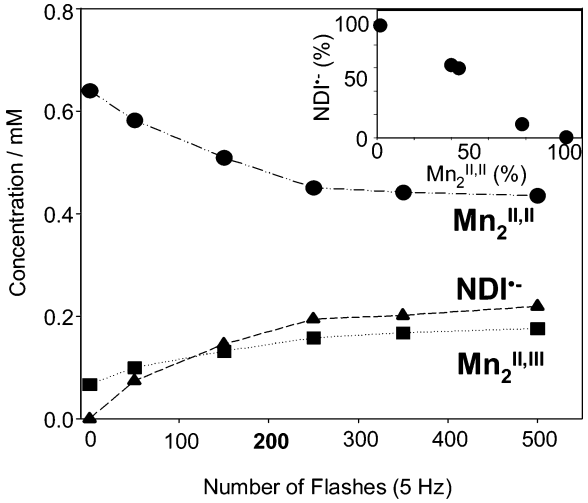

Figure 6. Plot showing change in concentration during laser flash photolysis at 140 K of $Mn_2^{II,II}$ (●), the $Mn_2^{II,III}$ (■), and the $NDI^{\bullet-}$ radical (▲) determined from EPR spectra. Data were taken from the experiment shown in Figure 5. The concentrations of $Mn_2^{II,II}$, $Mn_2^{II,III}$, and the $NDI^{\bullet-}$ radical were estimated as described in the Experimental Section. The inset shows that the decay of the $NDI^{\bullet-}$ radical (in the fraction of **1** where the radical was formed after the illumination) correlated to the regeneration of the $Mn_2^{II,II}$ state (also in the fraction of **1** where the manganese moiety was photo-oxidized) during an experiment when a sample of **1** that was provided 400 laser flashes at 140 K was incubated for various times at 140 K in the dark. The recombination between the $NDI^{\bullet-}$ radical and the $Mn_2^{II,III}$ was completed after ca. 30 min.

from the start, which would make the observed changes in $Mn_2^{II,III}$ smaller than immediately expected from the oxidation of $Mn_2^{II,II}$.

We also investigated if the oxidized $Mn_2^{II,III}$ dimer and the $NDI^{\bullet-}$ radical formed in the flash-photolysis experiment could recombine. For this purpose a sample was exposed to 400 flashes, which resulted in EPR signal changes as in Figure 5. This sample was then incubated at 140 K in the dark for some time after which it was cooled to 11 K and an EPR spectrum was recorded, where after it was heated to 140 K and further incubated. The signal changes due to generated $NDI^{\bullet-}$ and depleted $Mn_2^{II,II}$ were slowly reversed at 140 K, and after a total of 30 min in the dark at 140 K, the EPR spectrum recorded at 11 K was again identical to that of the original, unflashed sample (spectrum *i* of Figure 5a; not shown). A correlation study (Figure 6, inset) shows that the $NDI^{\bullet-}$ radical decay perfectly matched the regeneration of $Mn_2^{II,II}$, showing that a 1:1 recombination between the two product species is their main decay pathway. When the same sample was exposed to laser flashes once again, the $Mn_2^{II,II}$ signal intensity was found to decrease by 20% at saturation (compared to ca. 35% in the first experiment) with a corresponding increase of the $Mn_2^{II,III}$ as well as $NDI^{\bullet-}$ radical. A likely interpretation of this experiment is that the reaction to a large extent is reversible giving back the same starting state after charge recombination. However, the less efficient formation of the charge separated state in the second turn might indicate that a fraction of **1** had been modified in the complex experimental cycle, due to either the light exposure or the repeated freezing and thawing.

The recombination of the charge pair is faster at room temperature, and recombination was complete within the 2 min required to warm the sample (results not shown). Consequently,

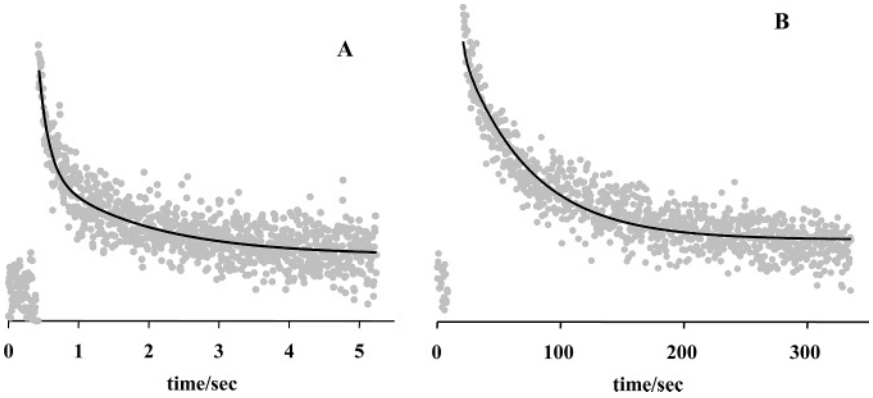

Figure 7. Formation and decay of the EPR signal intensity probing the $NDI^{\bullet-}$ radical after one flash (532 nm) given to the sample at 140 K, measured with two different time windows. The transient decay kinetics was recorded at 3344 G corresponding to the maximum EPR signal of the $NDI^{\bullet-}$ radical. The solid lines show the biexponential fit giving $\tau_1 = 140$ ms, $\tau_2 = 1.40$ s (A) and the single-exponential fit giving $\tau_3 = 122$ s (B). Note that the scales on the *x*-axes are different and that the fast phases are not seen on the time scale of the decay trace in panel B. EPR settings: microwave frequency, 9.62 GHz; modulation amplitude, 5 G; microwave power, 20 mW, $T = 140$ K.

attempts to trap charge separation products induced by flashing at room temperature and analyzing them by EPR were not successful.

The flash induced formation and recombination of the $NDI^{\bullet-}$ radical could also be followed with time-resolved EPR and optical spectroscopy (see below). For the EPR experiment, the magnetic field was positioned at the positive maximum of the $NDI^{\bullet-}$ radical signal (compare Figure 5c). A single laser flash, directed into the EPR cavity, generated the EPR signal from the $NDI^{\bullet-}$ radical within our time resolution (Figure 7). It decayed following multiexponential kinetics. The initial part of the decay curve obtained at 140 K (Figure 7a) could be fitted satisfactorily by a sum of two exponentials with $\tau_1 = 140$ ms ($A_1 = 0.55$) and $\tau_2 = 1.40$ s ($A_2 = 0.35$). In addition to these processes, a very slow component could be discerned from the kinetic trace. This component decayed with $\tau = 120-130$ s at 140 K (Figure 7b) and involved about 10% of the totally generated $NDI^{\bullet-}$ radical. The same kinetic behavior was found when the ruthenium was excited both at 532 nm, at the red edge of the MLCT band, and at 460 nm, at the maximum of the MLCT band (not shown). It is important to note that only the charge separated state originating from the slow phases could be picked up in our flash-freeze experiments aimed at studying the Mn-oxidation reaction. The reason is that the main part of the charge separated state, that decays already within a few seconds, would have recombined during our freezing procedure, which took 2 to 3 seconds.

Quantitative estimation revealed that the total yield of $NDI^{\bullet-}$ radical in each flash was ca. 1.3% of the total sample present. Thus, the slowest component ($\tau = 120-130$ s) corresponded to the formation of ca. 0.13% $NDI^{\bullet-}$ per flash. This is in good agreement with the fact that 250 flashes were required to achieve ca. 30% of $Mn_2^{II,II}$ oxidation in our flash-freeze experiment (Figure 5). In fact, a simulation of the accumulation experiments at 5 Hz excitation, assuming 0.13% $NDI^{\bullet-}$ formation per flash and a 120 s lifetime, agrees well with the data in Figure 5 (not shown).

It is interesting to discuss the origin of the slow phase. Aggregation involving π-stacking is known to occur for NDI- and perylene diimide-containing molecules.[27,28] This is a clear possibility also for **1**, in particular at low temperature. It has previously been found that the $NDI^{\bullet-}$ radical is very stable and inert to oxygen in some of these aggregates indicating that the aggregate can function as some form of hinder against radical oxidation.[27] If aggregates are formed in **1**, an electron can be delocalized over a large number of NDI molecules[28c] and thereby stabilize a fraction of the $NDI^{\bullet-}$ radicals making an even slower recombination at this temperature and these concentrations. Thus, even though aggregation might seem an unwanted complication, if this lies behind the very slow component it provided us with a tool to investigate the Mn-chemistry directly using flash-freeze methods and EPR spectroscopy.

There are several main conclusions from our EPR experiments. We observed formation and decay of the $NDI^{\bullet-}$ radical at 140 K. The radical decayed with several kinetic components. One of them lived on a minute time scale and might be due to aggregation of **1** via the NDI acceptor moiety. For this slow reaction we observed that $Mn_2^{II,II}$-oxidation accumulated in parallel with formation of the $NDI^{\bullet-}$ radical. The so formed charge pair was very stable at 140 K and decayed within 30 min in a process where the decay of $NDI^{\bullet-}$ and the regeneration of $Mn_2^{II,II}$ occurred in parallel. This indicates that no unknown species are involved in the reactions and is an important advantage to donor−acceptor systems where only one of the product species could be followed (see below). Consequently, we conclude that the triad **1** exhibits light-induced charge separation resulting in reduction of the NDI acceptor and oxidation of the $Mn_2^{II,II}$ moiety. This is the first time this has been demonstrated in a synthetically linked donor−sensitizer−acceptor triad containing a manganese complex as donor.

Although we could not follow the manganese oxidation with time-resolved EPR, there is no reason to suggest that the two faster decay reactions (decaying with $\tau = 140$ ms and 1.4 s) of the $NDI^{\bullet-}$ radical do not involve back-reactions with photooxidized manganese. This is supported by the optical spectroscopy results discussed below.

B. Optical Spectroscopy. With optical transient absorption spectroscopy we could follow the kinetics of the laser flash induced charge separation processes by the formation and decay of $NDI^{\bullet-}$, the decay of the ruthenium excited state, and the

(28) (a) Penneau, J.-F.; Stallman, B. J.; Kasai, P. H.; Miller, L. L. *Chem. Mater.* **1991**, *3*, 791−796. (b) van der Boom, T.; Hayes, R. T.; Zhao, Y.; Bushard, P. J.; Weiss, E. A.; Wasielewski, M. R. *J. Am. Chem. Soc.* **2002**, *124*, 9582−9590. (c) Rybtchinski, B.; Sinks, L. E.; Wasielewski, M. R. *J. Phys. Chem. A*, **2004**, *108*, 7497−7505.

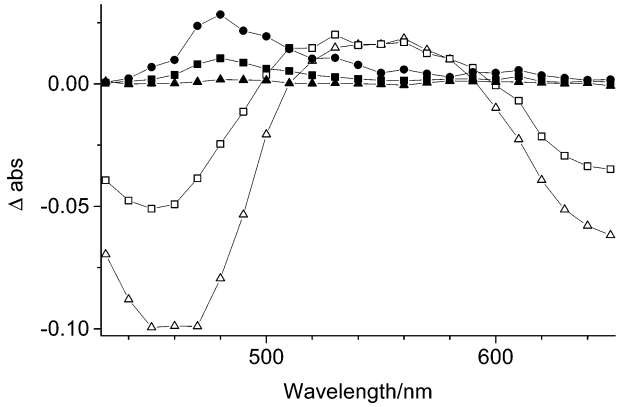

Figure 8. Transient absorption spectra of **1** taken at different times after excitation; 10 ns (△), 30 ns (□), 300 ns (●), 0.15 ms (■), and 4 ms (▲) (butyronitrile, 298 K, excitation at 455 nm).

presence or absence of an oxidized or reduced ruthenium intermediate. Electron transfer from the $Mn_2^{II,II}$ unit was probed indirectly by the oxidation states of the ruthenium moiety. In liquid butyronitrile the results were qualitatively similar in the temperature range 140−298 K and only the time constants varied. Below, detailed results are presented for the two extreme temperatures in that interval followed by a discussion about the recombination kinetics.

At 298 K the emission lifetime (τ) of **1** in CH_3CN was determined with time-correlated single photon counting. Compared to $[Ru(bpy)_3]^{2+}$ ($\tau \approx 1$ μs in deaerated CH_3CN)[20] the lifetime of **1** was strongly reduced and showed biexponential kinetics ($\tau_1 = 7$ ns, $A_1 = 0.25$ and $\tau_2 = 40$ ns, $A_2 = 0.75$). For complex **3** lacking the $Mn_2^{II,II}$ unit, we observed similar kinetics ($\tau_1 = 7$ ns, $A_1 = 0.15$ and $\tau_2 = 27$ ns, $A_1 = 0.85$). As we have argued above, we believe that the biexponential decay is due to the presence of different isomers. Since the quenching rate at 298 K is similar in **1** and **3**, we conclude that the NDI unit is the dominating quencher. This is in agreement with previous results in the $Mn_2^{II,II}$−Ru^{II} dyad ($[Ru(bpy)_3$−$Mn_2(bpmp)$-$(OAc)_2]^{3+}$), where the ruthenium excited state lifetime was longer (τ = 110 ns for the main component) and no photoproducts except the excited state could be detected by transient absorption.[13] The quenching of **1** could be due to both electron transfer and triplet energy transfer to the NDI unit as judged from the thermodynamics in Figure 4, where the former process has a larger driving force ($\Delta G° = -0.20$ eV) as compared to energy transfer ($\Delta G° = -0.02$ eV).

To investigate the initial quenching products of **1**, transient absorption spectra were obtained after excitation with a <10 ns laser flash at 455 nm, in both acetonitrile and butyronitrile at 298 K. The results were similar for the two solvents, while butyronitrile allowed temperature-dependent studies in fluid solvent down to 140 K. In Figure 8, the room temperature transient absorption spectra of **1** at different times after excitation are shown. The spectra show the decay of the initially formed ruthenium excited state, which is characterized by a bleaching around 450 nm ($\Delta\epsilon \approx 2.0 \times 10^4$ M^{-1} cm^{-1})[20,29] and an emission above 600 nm. After 300 ns a new spectrum with positive absorption peaks around 480 and 610 nm appeared. An identical spectrum is seen at 140 K after 10 μs and remained on the millisecond time scale (Figure 9b, inset). We attribute these spectral changes to formation of the reduced $NDI^{\bullet-}$, which has absorption maxima at 474 nm ($\epsilon = 2.6 \times 10^4$ M^{-1} cm^{-1}) and 605 nm ($\epsilon = 7.2 \times 10^3$ M^{-1} cm^{-1}).[25] From these data we conclude that the quenching mechanism is electron transfer.

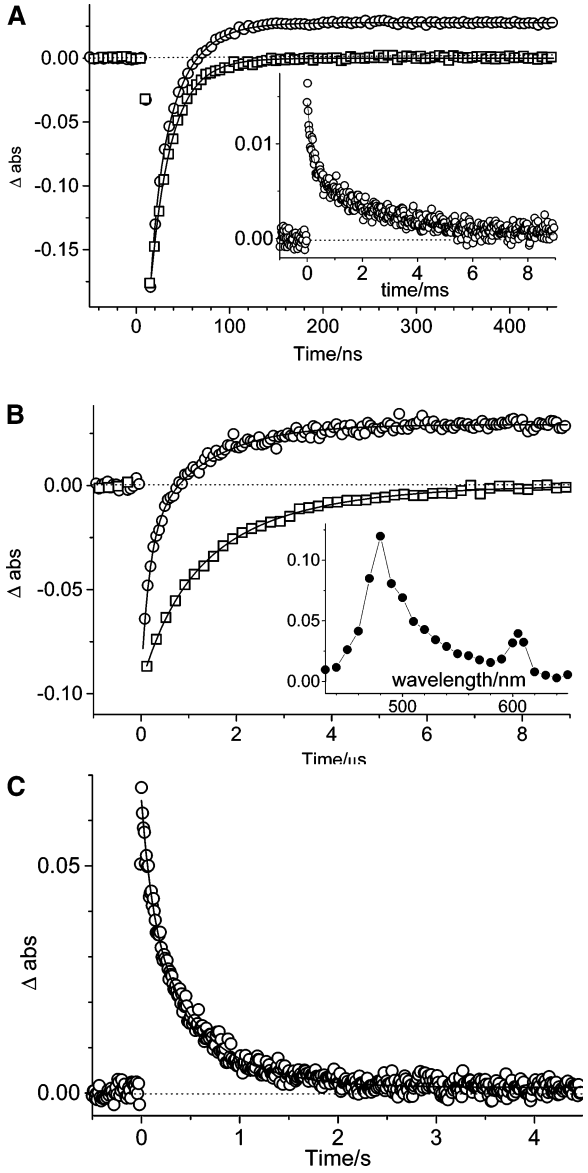

Figure 9. Transient absorption traces probed at 475 nm for **1** (circles) and **3** (squares), showing the decay of ruthenium excited state and formation of $NDI^{\bullet-}$ radical (A) at 298 K and (B) at 140 K, while panel C shows the subsequent decay of the long-lived $NDI^{\bullet-}$ radical at 140 K. The solid lines are fits of the data to a sum of exponentials (see text for results). The inset in panel B shows the transient absorption spectrum of **1** at 140 K, taken after 1 ms. The inset in panel A shows the decay of the $NDI^{\bullet-}$ absorption at 475 nm for **1** at room temperature, while the decay at 140 K (panel C) was much slower (see text). Conditions: 20 μM solutions in butyronitrile, excitation at 455 nm.

The recovery of the ruthenium ground state, measured from the bleaching around 450 nm, follows the same kinetics as the $NDI^{\bullet-}$ formation. A biexponential fit to the traces at 450 (not shown) and 475 nm (Figure 9a) gave $\tau_1 = 10$ ns[30] and $\tau_2 = 30$ ns at 298 K, in good agreement with the emission quenching

(29) Assuming an excited-state extinction coefficient similar to that for $[Ru(bpy)_3]^{2+}$. The $\Delta\epsilon$ value for **1** is twice that for $[Ru(bpy)_3]^{2+}$ due to the higher ground-state extinction coefficient.

(30) The accuracy of the first value was limited by the instrument and the presence of the short-lived emission in the butyronitrile solvent, which also made the estimation of relative amplitudes between the two time constants uncertain.

kinetics above. The reference dyad **3** gave a very similar result: $\tau_1 = 9$ ns and $\tau_2 = 25$ ns. At 140 K the corresponding time constants for **1** were $\tau_1 = 0.2\ \mu$s ($A_1 = 0.55$) and $\tau_2 = 1.2\ \mu$s ($A_1 = 0.45$), and similarly for **3**, they were $\tau_1 = 0.6\ \mu$s ($A_1 = 0.3$) and $\tau_2 = 2.0\ \mu$s ($A_1 = 0.7$) (Figure 9b). The fact that no long-lived Ru^{III} state is formed, as shown by the absence of Ru^{II} ground-state bleach, at either temperature suggests that a fast ($\tau < 30$ ns at 298 K) secondary electron-transfer step has to follow the initial photo-oxidation of Ru^{III}, regenerating the Ru^{II} state. In **3** this is obviously just a rapid recombination reaction, regenerating the ground state reactants. In **1** instead, the $NDI^{\bullet-}$ is long-lived and we propose the regeneration of Ru^{II} to be due to electron transfer from the $Mn_2^{II,II}$ unit, which is in accordance with the EPR results as well as with the previously shown rapid $Mn_2^{II,II}$-to-Ru^{III} electron transfer ($\tau < 100$ns) in the corresponding dyad.[13] The first oxidation of $Mn_2^{II,II}$ is manganese based, oxidizing the complex from the $Mn_2^{II,II}$ to the $Mn_2^{II,III}$ state.[12] Thus, although the optical absorption of these two redox states is too small to detect in the transient absorption experiments, our results allow us to conclude that the photo-induced reaction sequence is (cf. solid arrows in Figure 4):

$$Mn_2^{II,II}-Ru^{II}-NDI \xrightarrow{h\nu} Mn_2^{II,II}-{}^*Ru^{II}-NDI \rightarrow$$
$$\rightarrow Mn_2^{II,II}-Ru^{III}-NDI^{\bullet-} \rightarrow Mn_2^{II,III}-Ru^{II}-NDI^{\bullet-} \quad (2)$$

The quenching rates observed for the reference dyad **3** were very similar, at both 140 and 298 K, but no long-lived $NDI^{\bullet-}$ radical could be observed (Figure 9a and b). This shows that the charge recombination from $NDI^{\bullet-}$ to Ru^{III} is faster than the initial charge separation in **3**. Thus for **1**, it is likely that charge recombination and further charge shift to form $Mn_2^{II,III}-Ru^{II}-NDI^{\bullet-}$ compete, reducing the quantum yield of the fully charge separated state. The yield of the initially formed $Mn_2^{II,II}-Ru^{III}-NDI^{\bullet-}$ state should be high, ≈0.95, based on the emission quenching results. The quantum yield of the fully charge-separated state $Mn_2^{II,III}-Ru^{II}-NDI^{\bullet-}$ state was estimated by the relative magnitudes of the initial bleaching at 450 nm quantifying the ruthenium excited state by the ground state bleach and the maximum absorption at 480 nm quantifying the $NDI^{\bullet-}$ radical at its maximum concentration, using the difference extinction coefficients given above. The calculation gave $\phi_{CS} \approx 20\%$ at 298 K (10% in CH_3CN) and $\phi_{CS} \approx 40\%$ at 140 K.

The decay of the charge-separated state at 298 K, monitored at 475 nm (Figure 9a, inset), could be well fitted to a sum of three exponentials: $\tau_1 = 15\ \mu$s ($A_1 = 0.5$), $\tau_2 = 200\ \mu$s ($A_2 = 0.25$), and $\tau_3 = 2.3$ ms ($A_3 = 0.25$). The average lifetime is very long, at least 2 orders of magnitude longer than those for previously published triads based on $[Ru(bpy)_3]^{2+}$ chromophores.[9−11] This result is very interesting and will be further discussed in the next section. At 140 K the recombination was even slower reaching even up to the time scale of seconds (Figure 9c). A sum of two exponentials was sufficient for a good fit: $\tau_1 = 100$ ms ($A_1 = 0.45$) and $\tau_2 = 500$ ms ($A_1 = 0.55$) (Figure 9c). The deviation from single exponential kinetics is tentatively ascribed to different rates for the different isomers, as discussed above. The experiment could be repeated with hundreds of laser flashes on the same sample without any detectable decrease in the yield of $NDI^{\bullet-}$ or change in recombination kinetics. From this result we can calculate that each molecule generated the charge-separated state more than five times on the average without any detectable degradation. Thus, the long-lived charge separation is highly reversible. At 140 K the lifetimes for the decay of the $NDI^{\bullet-}$ radical were in good agreement with those found in the EPR experiment ($\tau_1 =$ 140 ms and $\tau_2 = 1.4$ s). However, we could not observe the small and very slow component decaying on the minute time scale in the EPR experiment (see above). This is possibly due to the lower concentrations used in the optical experiment. At higher concentration (50−60 μM), similar to that in the EPR experiments, there was no difference in room temperature transient absorption results compared to the experiments at ca. 20 μM. At 140 K, however the more concentrated samples turned strongly opaque (OD > 2 in the visible region), which precluded optical experiments. This may possibly be due to the formation of large aggregates of **1** and/or microcrystals of solid solvent, as 140 K is between the glass transition temperature (<120 K) and the freezing point (161 K). This observation might be related to the presence of the very slow ($\tau \approx 120$ s) $NDI^{\bullet-}$ decay phase observed in the EPR experiments, experiments which do not require transparency in the visible region.

The lifetime of the charge-separated state was long enough for intermolecular charge recombination to occur. This idea was coherent with the kinetic traces at 298 K, which could be reasonably well fitted also to a second-order decay. No change in the kinetics was observed when the initial concentration of the charge-separated state was varied between ca. 0.4 and 2 μM however, suggesting that intermolecular reactions were insignificant. To further rule out the possibility of intermolecular charge recombination, transient absorption experiments of **1** were performed in a PMMA solid matrix at 298 K. At the low concentration of **1** employed (≈20 μM), only intramolecular electron transfer may occur as diffusion is hindered. In PMMA the charge-separated state $Mn_2^{II,III}-Ru^{II}-NDI^{\bullet-}$ was formed with a yield $\phi \approx 0.25$ and the rate of charge recombination, $t_{1/2} \approx 30\ \mu$s, was similar to that in the solution phase (see Supporting Information). Together with the lack of concentration dependence above, this similarity shows that intermolecular charge recombination is not significant in solution. An interesting observation from the matrix experiments was that the dominating quenching mechanism of the ruthenium excited state was changed from electron transfer ($^*Ru^{II}-NDI \rightarrow Ru^{III}-NDI^{\bullet-}$) in liquid butyronitrile to energy transfer ($^*Ru^{II}-NDI \rightarrow Ru^{II}-{}^{*3}NDI$) in the matrix (see Supporting Information). The $^{*3}NDI$ state then generated the same charge separated state as that observed in the liquid. The change to energy transfer could be explained by the fact that solvent repolarization, stabilizing charge transfer states, was hindered in the solid state. This generally makes electron transfer less energetically favorable, as has been discussed for low-temperature glasses,[31] while energy transfer reactions are much less affected. Note also that transient absorption experiments performed on **1** in butyronitrile glass at 80 K showed that electron transfer was blocked, and instead energy transfer to generate the ^3NDI occurred (not shown).

Analysis of the Recombination Kinetics. One long-standing goal of artificial photosynthesis is to generate charge-separated

(31) (a) Wasielewski, M. R.; Johnson, D. G.; Svec, W. A.; Kersey, K. M.; Minsek, D. W. *J. Am. Chem. Soc.* **1988**, *110*, 7219−7221. (b) Gaines, G. L.; O'Neil, M. P.; Svec, W. A.; Niemczyk, M. P.; Wasielewski, M. R. *J. Am. Chem. Soc.* **1991**, *113*, 719−721. (c) Chen, P.; Meyer, T. J. *Inorg. Chem.* **1996**, *35*, 5520−5524

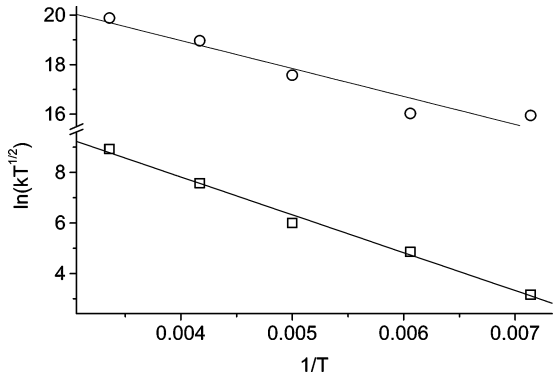

Figure 10. Marcus plot showing the temperature dependence of the rate constant ($\ln(kT^{1/2}) = f(T^{-1})$). Data for the primary charge separation reaction ($Mn_2^{II,II}$–*Ru^{II}–NDI → $Mn_2^{II,II}$–Ru^{III}–$NDI^{\bullet-}$) are marked with circles, and data for the recombination ($Mn_2^{II,III}$–Ru^{II}–$NDI^{\bullet-}$ → $Mn_2^{II,II}$–Ru^{II}–NDI) are marked with squares.

states long-lived enough that catalytic reactions can compete with charge recombination, so that conversion into stable products can be achieved. In Photosystem II the water oxidation of the manganese cluster is slow; the final oxidation of the cluster and release of O_2 occur with an overall time constant as long as ca. 1 ms.[2] Nevertheless, the catalytic conversion is efficient due to the very long lifetime of the Mn_{ox}–$Q_B^{\bullet-}$ charge-separated state.

The charge-separated state of the triad **1** is surprisingly long-lived, in particular at 140 K. Similarly long-lived charge separated states have recently been reported in low-temperature benzonitrile solutions of a porphyrin-based tetrad ($\tau = 1.6$ s at 163 K),[8b] a Zn-chlorin–fullerene dyad ($\tau = 150$ s at 123 K),[32] and a mesityl–methylacridinium dyad ($\tau = 2$ h at 203 K).[33] Very recently, however, Benniston et al.[34] concluded that the methylacridinium radical observed in the latter system was due to the presence of a sacrificial donor, presumably in the benzonitrile solvent, implying that the real charge separated state was not observed on these long time scales. Thus, observation of the reduced acceptor (fullerene or methylacridinium in the cases above) may not be sufficient as the only proof for the presence of an intramolecular charge separated state under those conditions. In this context, it is important to point out that we in our present study observe and follow the recombination of both the acceptor and donor species in a 1:1 ratio by EPR. In addition, we obtained the same $NDI^{\bullet-}$ decay kinetics in both molecular sieve-dried butyronitrile and in the same solvent distilled over P_2O_5, both at room temperature and at 140 K. Thus, we observe a genuine charge separated state in **1** with a very long lifetime.

It is interesting to note that already at room temperature the average lifetime is at least 2 orders of magnitude longer than that in previously reported donor–sensitizer–acceptor triads based on Ru(II)–polypyridine complexes.[9−11] To understand this favorable property, we studied the temperature dependence of the electron-transfer rates in more detail. Figure 10 shows the rate constants both for the initial quenching of the excited ruthenium and for the charge recombination at different temperatures from 140 to 298 K, plotted according to the Marcus' expression[35] in eq 3:

$$\ln(k_B T^{1/2}) = \ln\left(\frac{2\pi}{\hbar} H^2 (4\pi\lambda)^{-1/2}\right) - \frac{(\Delta G^\circ + \lambda)^2}{4\lambda k_B T} \qquad (3)$$

In the equation, H is the electronic coupling and λ is the reorganization energy.

The agreement between the data and the prediction of eq 3 is good. In Figure 10 the rate constants used are the slowest component from the time-resolved transient absorption experiments. The plots were qualitatively similar when instead an amplitude-weighted mean of the time constants was used, giving no significant difference in the slopes from those in Figure 10 (see Supporting Information). Both the primary charge separation and the recombination gave similar activation free energies: $\Delta G^{\#} = 0.09$ and 0.12 eV, respectively. Using these activation free energies and the driving force for the charge separation and recombination reaction ($\Delta G^\circ = -0.20$ eV and -1.07 eV, respectively), the reorganization energies were calculated from eq 3. For the forward electron transfer *Ru^{II}–NDI → Ru^{III}–$NDI^{\bullet-}$ the value obtained, $\lambda \approx 0.8$ eV, is typical for electron transfer in polar solvents in which most of the reorganization energy derives from the solvent.[35] In contrast, the reorganization energy for the recombination reaction $Mn_2^{II,III}$–Ru^{II}–$NDI^{\bullet-}$ → $Mn_2^{II,II}$–Ru^{II}–NDI is remarkably high: $\lambda \approx 2.0$ eV. This suggests a large inner reorganization contribution from the manganese complex of approximately 1.0 eV.

The inner reorganization energy λ_{in} is given by

$$\lambda_{in} = {}^1/_2 \Sigma k_i \Delta q_i^2 \qquad (4)$$

where k_i is the force constant for the ith inner vibration and Δq_i is the corresponding difference in equilibrium nuclear coordinates. We inspected the crystal structures of $[Mn_2(bpmp)OAc_2]^+$ and $[Mn_2(bpmp)OAc_2]^{2+}$ [12b,16a] to see if the magnitude of the nuclear displacements was large enough to be consistent with the high inner reorganization energy suggested by our data. The most important structural changes between the $Mn_2^{II,II}$ and $Mn_2^{II,III}$ states were observed for the metal ion–ligand distances of the manganese that changes oxidation states (see Table S1, Supporting Information). This Mn–O(phenoxy) distance changed by 0.214 Å. The Mn–O force constants for some Mn^{III}(μ-oxo) complexes have been determined to ca. 300 Nm^{-1}.[36] If we assume a somewhat smaller value of 200 Nm^{-1} for the Mn–O(phenoxy) bonds, the change in this bond distance alone nevertheless makes up for 0.29 eV of λ_{in}. For the remaining five Mn–ligand bonds of this manganese ion, the rms average Δq_i is 0.18 Å. Even if we assume an average force constant of only 100 Nm^{-1}, these still contribute an additional ca. 0.5 eV to λ_{in}. The contribution from the remaining bond changes, mainly those of the four acetate C–O distances, can be estimated to approximately 0.2 eV. Together these estimated contributions add up to ca. 1.0 eV. This result depends strongly on the significant bond length changes that are determined from the

(32) Ohkubo, K.; Kotani, H.; Shao, J.; Ou, Z.; Kadish, K. M.; Li, G.; Pandey; R. K.; Fujitsuka, M.; Ito, O.; Imahori, H.; Fukuzumi, S. *Angew. Chem., Int. Ed.* **2004**, 43, 853–855.
(33) Fukuzumi, S.; Kotani, H.; Ohkubo, K.; Ogo, S.; Tkachenko, N. V.; Lemmetyinen, H. *J. Am. Chem. Soc.* **2004**, *126*, 1600–1601.
(34) Benniston, A. C.; Harriman, A.; Li, P.; Rostron, J. P.; Verhoeven, J. W. *Chem. Commun.* **2005**, 2701–2703.
(35) Marcus, R. A.; Sutin, N. *Biochim. Biophys. Acta* **1985**, *811*, 265–322.
(36) (a) Sheats, J. E.; Czernuszewicz, R. S.; Dismukes, G. C.; Rheingold, A. L.; Petrouleas, V.; Stubbe, J.; Armstrong, W. H.; Beer, R. H.; Lippard, S. J. *J. Am. Chem. Soc.* **1987**, *109*, 1435–1444. (b) Visser, H.; Dubé, C. E.; Armstrong, W. H.; Sauer, K.; Yachandra, V. K. *J. Am. Chem. Soc.* **2002**, *124*, 1108–11017.

crystal structures and enter quadratically into eq 4, while it is less sensitive to errors in our guesses of force constants.

To conclude, our estimates based on the structural differences of the complex in the $Mn_2^{II,II}$ and $Mn_2^{II,III}$ state support our conclusion from the temperature-dependent data that the reorganization energy for the charge recombination reaction is high due to a large inner reorganization ($\lambda_{in} \approx 1.0$ eV) of the manganese complex. We have previously found similar values for the inner reorganization energies in a series of $Ru^{II}-Mn^{II}$ complexes, with mononuclear manganese complex moieties.[37] Most manganese complexes will probably display a large reorganization energy, at least between the Mn^{II} and the Mn^{III} states, due to the large differences in metal to ligand bond lengths in the two oxidation states. Note that also the preceding photo-oxidation of $Mn_2^{II,II}$ by Ru^{III} would then be expected to show a large reorganization energy. As the initial photo-oxidation of the excited Ru^{II} unit by the NDI was the rate-limiting step in charge separation, however, this was not possible to verify. The fact that the $Mn_2^{II,II}$ oxidation is still very rapid compared to the final recombination with $NDI^{\bullet-}$ can be explained by the much shorter electron transfer distance for the reaction with the ruthenium center than with the remote NDI units. This is expected to more than compensate for the somewhat lower driving force for the Ru^{III}-to-$Mn_2^{II,II}$ electron transfer ($\Delta G^\circ = -0.8$ eV; see Figure 4).

A well recognized strategy to obtain a slow recombination reaction in light-induced charge separation is, in addition to increasing the charge separation distance, to obtain a driving force larger than the reorganization energy ($-\Delta G^\circ > \lambda$, eq 3) so that the recombination reaction occurs in the Marcus inverted region.[35,38] However, the rate reduction in the inverted region is smaller than that predicted by the classical eq 3, due to nuclear tunneling.[35,38,39] It is interesting to note that while charge recombination in previous triads (see, e.g., refs 7−11) have occurred in the inverted or the near-activationless regimes, the present triad **1** is as far as we are aware the first in which charge recombination occurs far down in the Marcus normal region ($-\Delta G^\circ < \lambda$) while the energy of the charge separated state is still high ($-\Delta G^\circ = 1.07$ eV and $\lambda = 2.0$ eV for the charge recombination reaction). This situation is possible because of the unusually large reorganization energy of the manganese complex. As a consequence the recombination reaction is strongly activated and unusually slow for a Ru^{II}-based triad, with an amplitude-weighted average lifetime of ca. 600 μs at room temperature. Due to the high activation energy, the lifetime in **1** then becomes even much longer at 140 K, reaching a time scale comparable with those displayed by photosynthetic reaction centers at room temperature. The activation free energy $\Delta G^{\#} = 0.12$ eV determined above gives an exponential factor in eq 3 at 298 K of ca. 0.01, which explains most of the 2 to 3 orders of magnitude longer lifetime compared to the previously reported Ru-based triads.

For light-induced water splitting with molecular catalysts, the catalytic reaction steps will most likely be slow, as in the case of Photosystem II, because of the bond rearrangements of the substrate water. This puts high demands on a long-lived charge separation to allow the catalytic reactions to occur. Our conclusions suggest that manganese complexes to some extent carry their own solution to this problem. They display a high intrinsic reorganization energy, even in a simple electron transfer reaction as in the case of **1** where no substrate bond breaking or formation is involved. This will make recombination reactions slow also from charge separated states with a high energy. The triad **1** is the first in which a manganese complex, a potential water-oxidation catalyst, is used as an electron donor to obtain a light-induced charge-separated state. This new strategy to obtain a long-lived charge separation is interesting and will be further explored.

Conclusions

We have described the first synthetically linked electron donor−sensitizer−acceptor triad in which a manganese complex plays the role of the donor. Our data revealed the details of the light-induced charge separation processes and showed directly the formation of the products: the oxidized $Mn_2^{II,III}$ dimer complex $[Mn_2(bpmp)(OAc)_2]^{2+}$ and the reduced naphthalene-diimide ($NDI^{\bullet-}$) acceptor moieties. This charge separated state is very long-lived, with an amplitude-weighted average lifetime of ca. 600 μs in room temperature solution, which is at least 2 orders of magnitude longer than those for previously reported triads based on a $[Ru(bpy)_3]^{2+}$ photosensitizer. In fluid butyronitrile at 140 K, this intramolecular recombination was dramatically slowed, displaying a lifetime of 0.1−1 s, which is comparable to many of the naturally occurring charge-separated states in photosynthetic reaction centers. We found that the long lifetime to a large extent is explained by an unusually large reorganization energy ($\lambda \approx 2.0$ eV) for the recombination reaction, due to a large inner reorganization of the manganese complex, which makes the reaction strongly activated despite the large driving force for recombination ($-\Delta G^\circ = 1.07$ eV). Thus, the intrinsic properties of the manganese complex are favorable for creating a long-lived charge separation in the "Marcus normal region" (where $-\Delta G^\circ < \lambda$) also with a large energy content of the charge separated state. This makes further work with manganese complexes as donor components in triads very promising, aiming to utilize the long lifetime of the charge separated state. In particular it is interesting that we earlier, using the same Mn_2 dimer but in its free form or linked to a ruthenium complex, and using an exogenous electron acceptor, were able to observe three consecutive single step photo-oxidations of the Mn moiety.[14] Thus, in the triad **1**, where two NDI-acceptors are present it might in principle be possible to obtain a second chain of electron transfer reactions, going beyond the single-electron level. In addition, the very long-lived charge pair might allow also secondary reactions to be involved. Both these options make the complex **1** a useful mimic of charge separation in PS II involving the $CaMn_4$ cluster.

Acknowledgment. Jonas Bergquist (Analytical chemistry, Uppsala University) is gratefully acknowledged for providing the ESI-MS data. We are grateful for valuable discussions with Joakim Högblom, Dr. Ping Huang, and Dr. Reiner Lomoth and to Jihu Su, Henriette Wolpher, and Licheng Sun for their involvement in the early parts of these studies. This work was supported by the Swedish Energy Agency, The Swedish Research Council, DESS, The Swedish Foundation for Strategic

(37) Abrahamsson, M.; Berglund-Baudin, H.; Tran, Å.; Philouze, C.; Berg, K. E.; Raymond-Johansson, M. K.; Licheng, Sun.; Åkermark, B.; Styring, S.; Hammarström, L. *Inorg. Chem.* **2002**, *41*, 1534−1544.
(38) Closs, G. L.; Miller, J. R. *Science* **1988**, *240*, 440−446.
(39) Bixon, M.; Jortner, J. Electron Transfer − From Isolated Molecules to Biomolecules. In *Advances in Chemical Physics, Volume 106*; Prigogine, I.; Rice, S. A., Ed.; Wiley: 1999.

Research (SelKem), The Royal Swedish Academy of Sciences, The Knut and Alice Wallenberg Foundation, and NEST-STRP, SOLAR-H (EU Contract No. 516510).

Supporting Information Available: Experimental details and transient absorption data for experiments performed in PMMA and butyronitrile at 80 K, a plot of the temperature dependence of recombination based on the weighted average lifetime, and a table of crystallographic manganese−ligand distances in $[Mn_2(bpmp)OAc_2]^+$ and $[Mn_2(bpmp)OAc_2]^{2+}$. This material is available free of charge via the Internet at http://pubs.acs.org.

JA055243B